Biomaterials 33 (2012) 6172–6185

Contents lists available at SciVerse ScienceDirect

Biomaterials

journal homepage: www.elsevier.com/locate/biomaterials

Cancer cell labeling and tracking using fluorescent and magnetic nanodiamond

Zhi-Yi Lien [a], Tzu-Chia Hsu [a], Kuang-Kai Liu [b], Wei-Siang Liao [a], Kuo-Chu Hwang [c], Jui-I. Chao [a,b,*]

[a] Institute of Molecular Medicine and Bioengineering, National Chiao Tung University, Hsinchu 30068, Taiwan
[b] Department of Biological Science and Technology, National Chiao Tung University, Hsinchu 30068, Taiwan
[c] Department of Chemistry, National Tsing Hwa University, Hsinshu 300, Taiwan

ARTICLE INFO

Article history:
Received 23 March 2012
Accepted 5 May 2012
Available online 5 June 2012

Keywords:
Fluorescent and magnetic nanodiamond
Nanodiamond-bearing cancer cells
Flow cytometer
Magnetic device
Confocal microscope

ABSTRACT

Nanodiamond, a promising carbon nanomaterial, develops for biomedical applications such as cancer cell labeling and detection. Here, we establish the nanodiamond-bearing cancer cell lines using the fluorescent and magnetic nanodiamond (FMND). Treatment with FMND particles did not significantly induce cytotoxicity and growth inhibition in HFL-1 normal lung fibroblasts and A549 lung cancer cells. The fluorescence intensities and particle complexities were increased in a time- and concentration-dependent manner by treatment with FMND particles in lung cancer cells; however, the existence of FMND particles inside the cells did not alter cellular size distribution. The FMND-bearing lung cancer cells could be separated by the fluorescent and magnetic properties of FMNDs using the flow cytometer and magnetic device, respectively. The FMND-bearing cancer cells were identified by the existence of FMNDs using flow cytometer and confocal microscope analysis. More importantly, the cell morphology, viability, growth ability and total protein expression profiles in the FMND-bearing cells were similar to those of the parental cells. The separated FMND-bearing cells with various generations were cryopreservation for further applications. After re-thawing the FMND-bearing cancer cell lines, the cells still retained the cell survival and growth ability. Additionally, a variety of human cancer types including colon (RKO), breast (MCF-7), cervical (HeLa), and bladder (BFTC905) cancer cells could be used the same strategy to prepare the FMND-bearing cancer cells. These results show that the FMND-bearing cancer cell lines, which reserve the parental cell functions, can be applied for specific cancer cell labeling and tracking.

1. Introduction

The use of nanomaterials in biomedical applications is of great interest since their size scale is similar to biological molecules and structures [1,2]. Many nanomaterials such as quantum dots (QDs) [2], gold nanobeads [3], and silica nanoparticles [4] have been developed for biomedical applications. The fluorescent molecules were covalently linked to iron oxide nanoparticles that used for the dynamic tracking of human stem cells [5]. Furthermore, the human induced pluripotent stem cells (iPS) can be generated by using polyamidoamine dendrimer-modified magnetic nanoparticle as the transfection system for *in vivo* imaging and tracking [6]. Besides, the silicon QDs can be used as fluorescent probes for tumor vasculature targeting, sentinel lymph node mapping, and multicolor near infrared imaging in live mice [4]. In addition to bio-labeling and -imaging, nanoparticles were studied for carrying drugs in cancer therapies [7–9].

Nanodiamond (ND), a carbon derivative nanomaterial has become a promising candidate in biological applications [10–15]. As substitutes for the aforesaid nanomaterials, ND is a nanomaterial applicable in the biomedical field, due to its excellent biocompatibility as compared with other nanoscale carbon materials. It has been corroborated that ND can be used in many cell lines without obvious cytotoxicity such as lung [16,17], neuronal [18], renal [19], and cervical cells [20,21]. Moreover, ND did not lead to obvious abnormality in cell division, differentiation and morphological changes in embryonic development [17,22].

ND has several advantages from its electrochemical and optical properties. Biological molecules or therapeutic agents can be provided, either by chemical modification of NDs, or by allowing physical attachment to NDs, which acts as a convenient binding platform for chemical agents. The surface functionalized ND particles have been shown to conjugated with fluorescent molecules [18,21,23–25], DNA [26], siRNA [27], proteins [28–30],

* Corresponding author. Department of Biological Science and Technology, National Chiao Tung University, 75, Bo-Ai Street, Hsinchu 30068, Taiwan. Tel.: +886 3 5712121; fax: +886 3 5556219.
E-mail address: jichao@faculty.nctu.edu.tw (J.-I. Chao).

0142-9612/$ – see front matter © 2012 Elsevier Ltd. All rights reserved.
doi:10.1016/j.biomaterials.2012.05.009

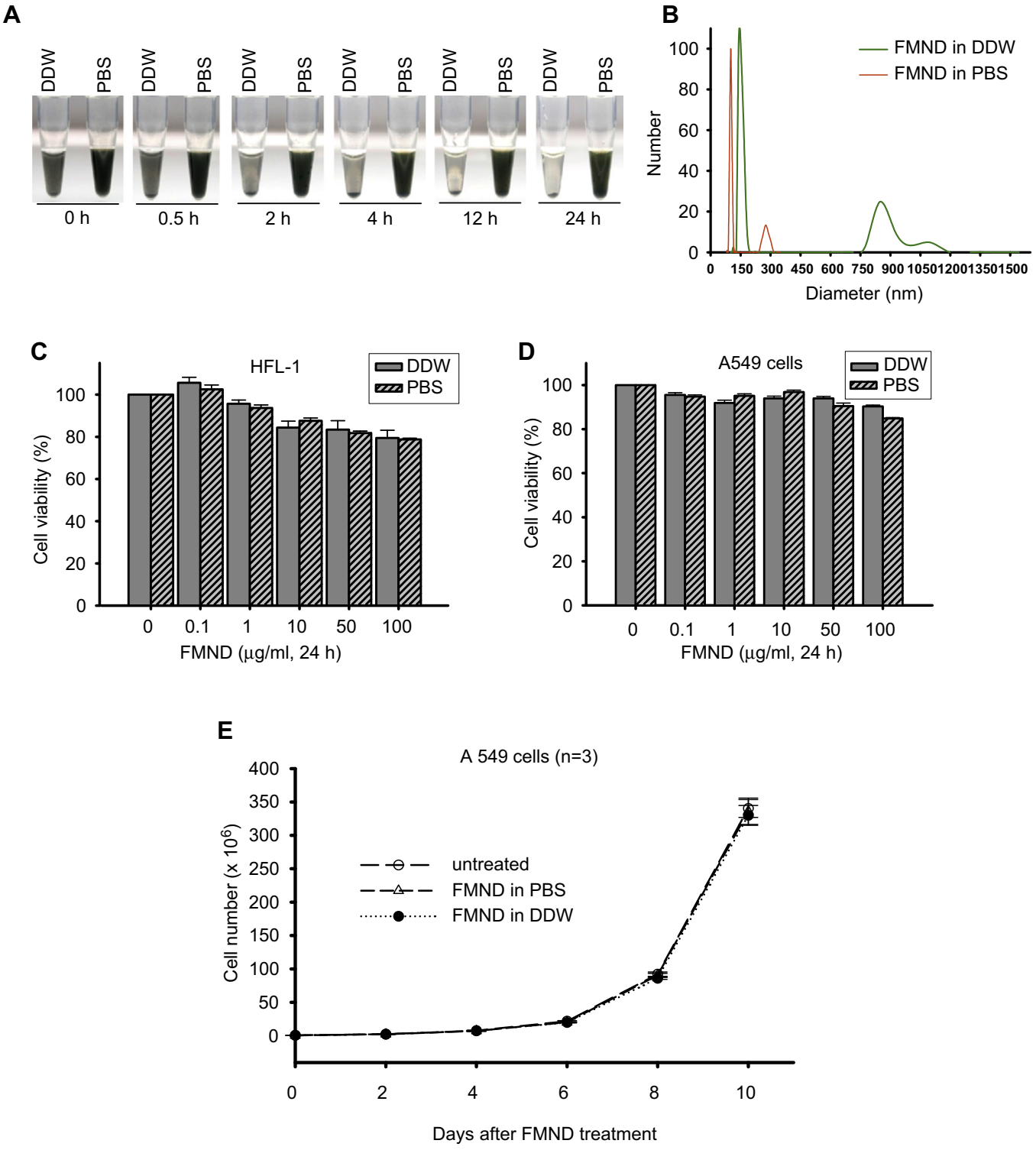

Fig. 1. Effect of cell viability and growth ability by treatment with FMND particles in human lung normal fibroblast and lung cancer cells. (A) Distilled deionized water (DDW) or phosphate-buffered saline (PBS) were used as solvent for FMND particles. The stock solution of FMND particles was 2.1 mg/ml. The equal volume of 100 μl FMND solution in DDW or PBS was added in 0.5 ml eppendorf tube, and stayed for 0–24 h observation. (B) The concentration of 0.5 mg/ml FMND particles in DDW or PBS was prepared by dynamic light scattering (DLS) analysis. The green picks indicate the size distribution of FMNDs in DDW. The orange picks indicate the size distribution of FMNDs in PBS. The effects of FMNDs on the cell viability in HFL-1 normal lung fibroblasts (C) and A549 lung carcinoma cells (D) were measured by MTT assays. The cells were treated with or without FMND (0.1–100 μg/ml for 24 h). Results were obtained from three separate experiments and the bar represents mean ± S.E. (E) A549 cells were plated at a density of 1×10^6 cells/100-mm Petri dish for 24 h, and then the cells were incubated with or without 50 μg/ml of FMNDs for 24 h. The cells were re-cultured in fresh medium for counting the total cell number by every 2 days until total 10 days. Results were obtained from three separate experiments and the bar represents the mean ± S.E. (For interpretation of the references to color in this figure legend, the reader is referred to the web version of this article.)

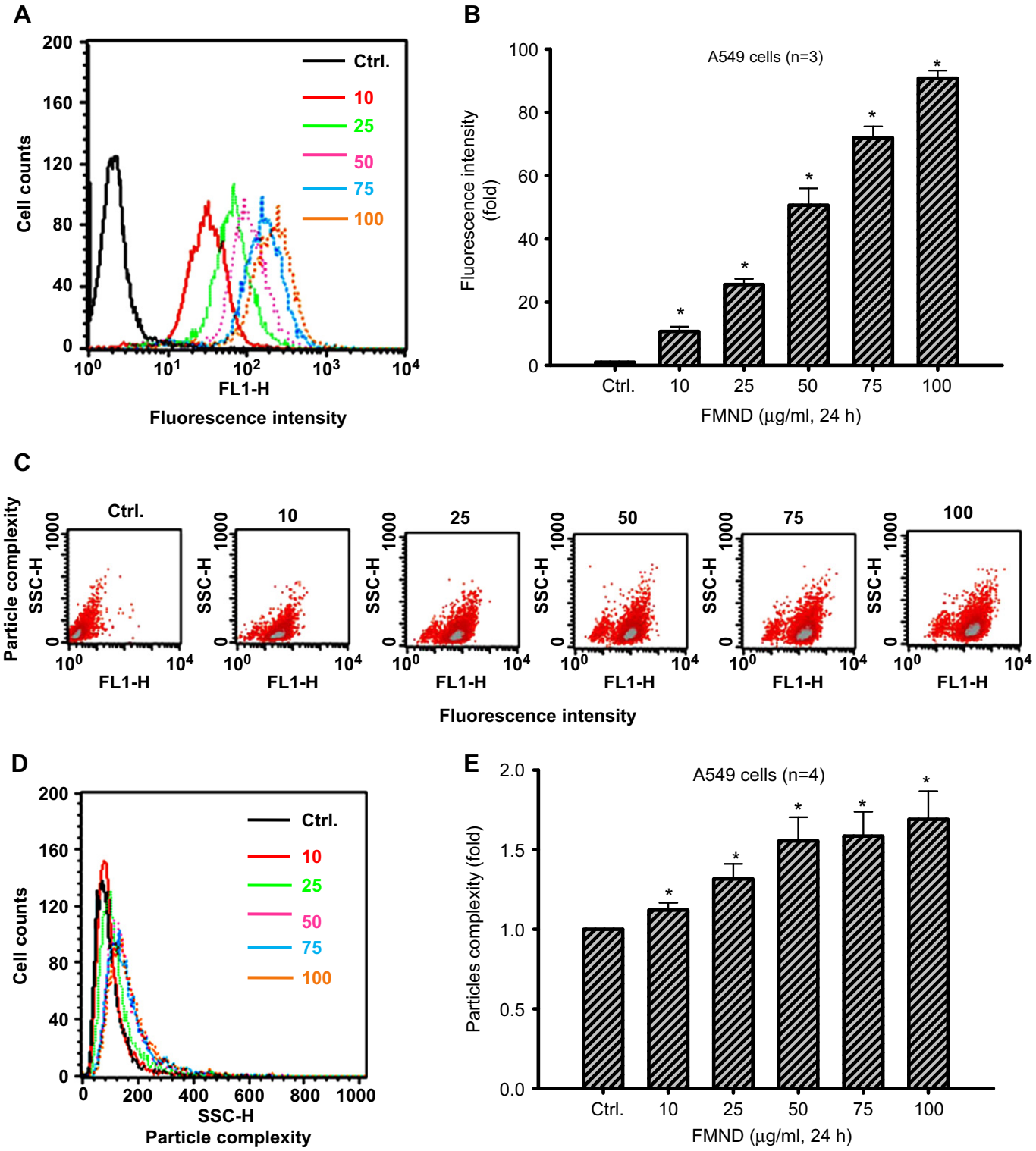

Fig. 2. Fluorescence intensity and particle complexity of FMND particles inside A549 lung carcinoma cells in a concentration-dependent manner. (A) The cells were incubated with 0–100 μg/ml FMNDs for 24 h. At the end of treatment, the cells were trypsinized and then subjected to flow cytometer analysis. *Y*-axis indicates the cell counts. The fluorescence intensity from FMND was excited with wavelength 488 nm, and the emission was collected in 515–545 nm signal range (FL1-H). (B) The fluorescence intensity was quantified from a minimum of 10,000 cells by CellQuest software. Results were obtained from three separate experiments and the bar represents mean ± S.E. $^*p < 0.05$ indicates significant difference between untreated and FMND-treated samples. (C) The cells were incubated with 0–100 μg/ml FMNDs for 24 h. The fluorescence intensity from FMNDs was excited with wavelength 488 nm, and the emission was collected in 515–545 nm signal range (FL1-H). SSC-H indicates the particle's complexity. (D) *Y*-axis indicates the cell counts. SSC-H indicates the particle's complexity. (E) The particle complexity of SSC-H was quantified from a minimum of 10,000 cells by CellQuest software. Results were obtained from three separate experiments and the bar represents mean ± S.E. $^*p < 0.05$ indicates significant difference between untreated and treated samples.

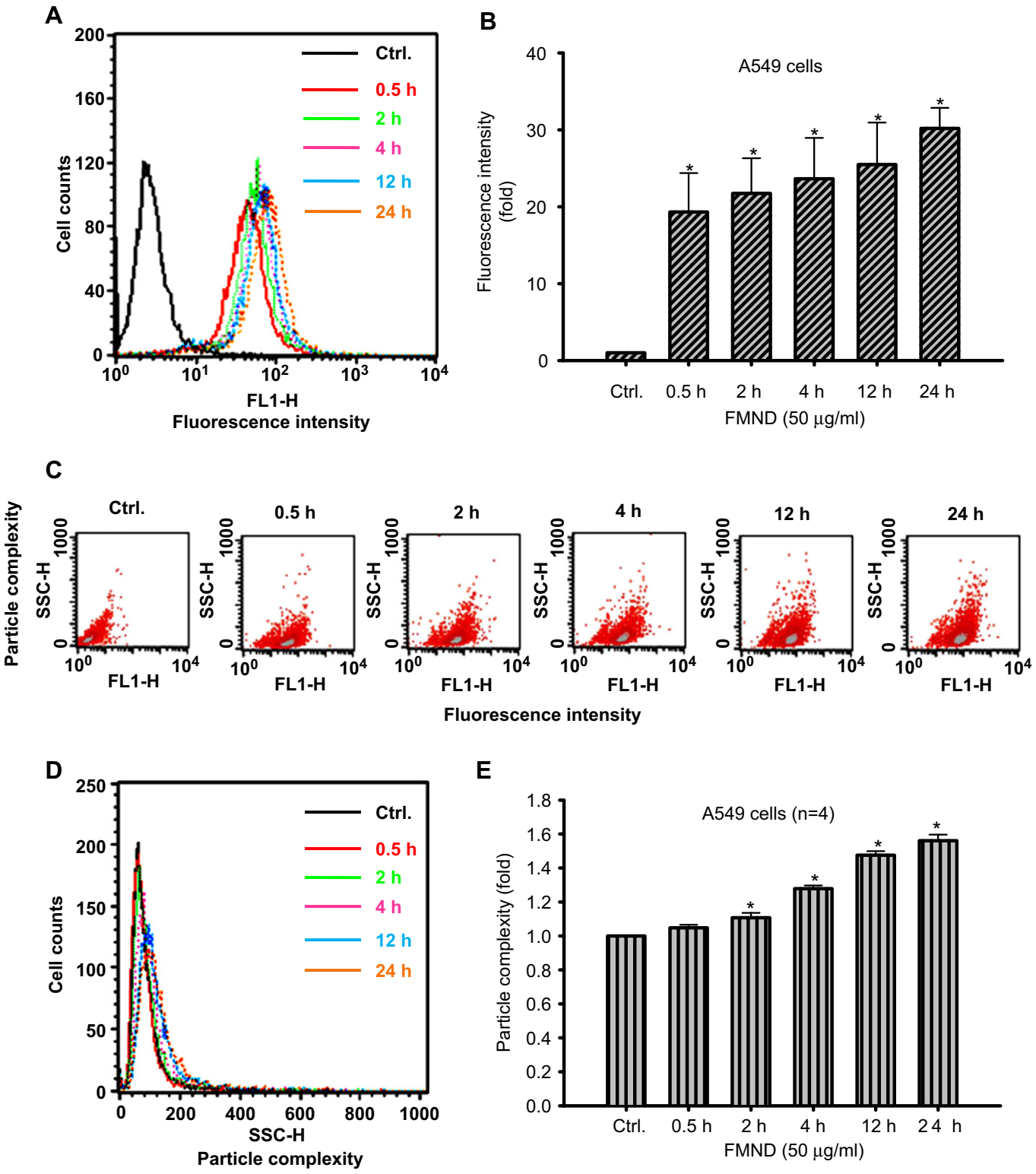

Fig. 3. Fluorescence intensity and particle complexity of FMND in A549 cells via a time-dependent manner. (A) The cells were incubated with or without 50 μg/ml FMNDs for 0–24 h. At the end of treatment, the cells were trypsinized and then subjected to flow cytometer analysis. *Y*-axis indicates the cell counts. The fluorescence intensity from FMND was excited with wavelength 488 nm and the emission was collected in 515–545 nm signal range (FL1-H). (B) The fluorescence intensity was quantified from a minimum of 10,000 cells by CellQuest software. Results were obtained from three separate experiments and the bar represents mean ± S.E. $^{*}p < 0.05$ indicates significant difference between untreated and treated samples. (C) The cells were incubated with or without 50 μg/ml FMNDs for 0–24 h. The fluorescence intensity from FMNDs was excited with wavelength 488 nm, and the emission was collected in 515–545 nm signal range (FL1-H). SSC-H indicates the particle's complexity. (D) *Y*-axis indicates the cell counts. SSC-H indicates the particle's complexity. (E) The particle complexity of SSC-H was quantified from a minimum of 10,000 cells by CellQuest software. Results were obtained from three separate experiments and the bar represents mean ± S.E. $^{*}p < 0.05$ indicates significant difference between untreated and treated samples.

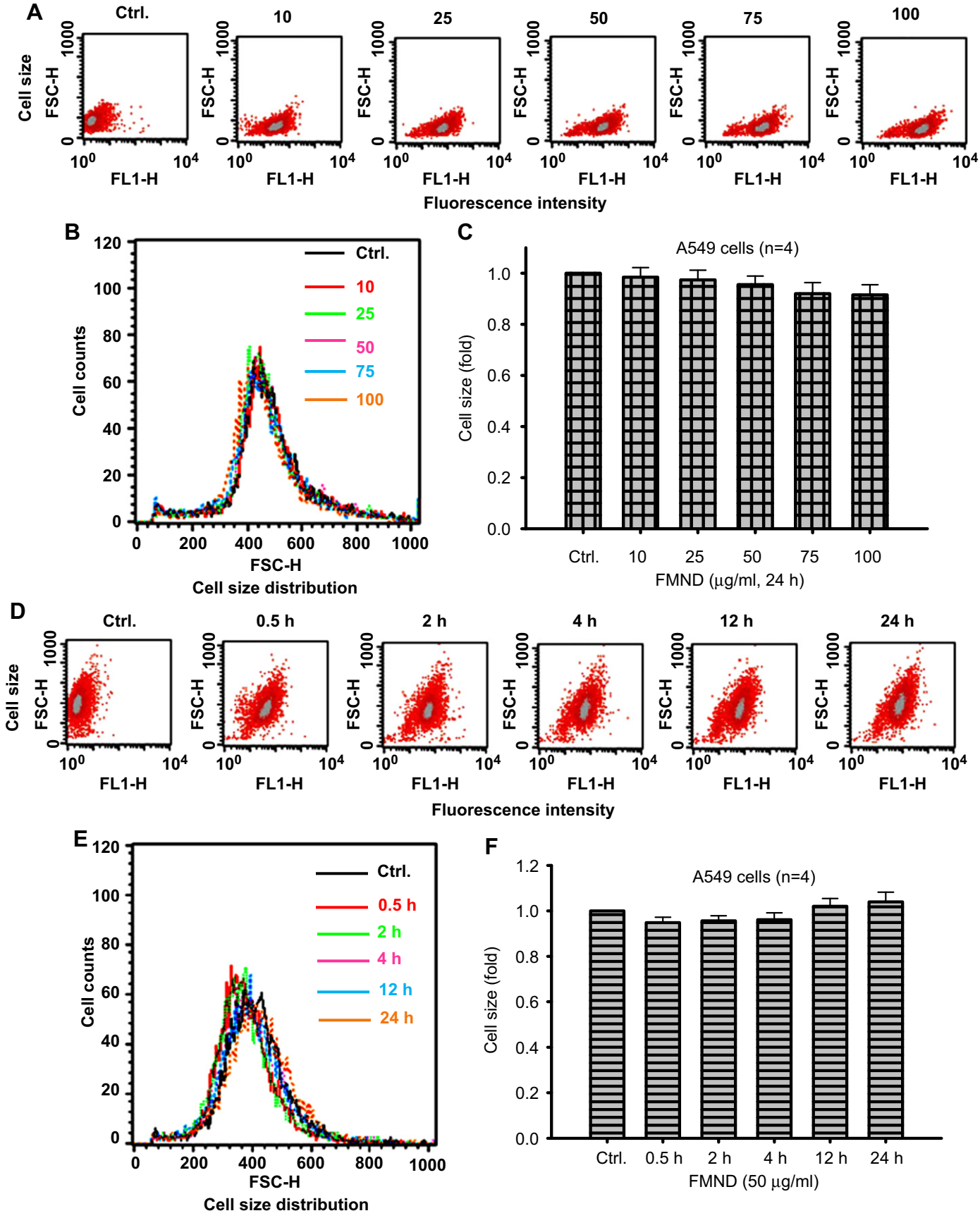

Fig. 4. Cell size distribution of A549 cells did not alter following exposure to FMND particles. (A) The cells were incubated with 0–100 μ g/ml FMND for 24 h. At the end of treatment, the cells were trypsinized and then subjected to flow cytometer analysis. The fluorescence intensity from FMND was excited with wavelength 488 nm and the emission

lysozyme [31], growth hormone [32], cytochrome *c* [33], alcohol dehydrogenase [34], antibodies [35,36], anti-cancer drugs [37–40], and dopamine derivatives [41].

ND can emit bright fluorescence, and does not bring about photobleaching [19,31]. Also, the fluorescent property can be introduced to an ND by binding a fluorescent molecule to the ND surface [18,21,23,24]. For example, the aminated NDs, ND-NH_2, are coupling to the reactive N-hydroxysuccinimide functionalized tetramethylrhodamine (TAMRA) to form TAMRA-ND [18,25]. TAMRA-ND complex is a high stable fluorescent probe to be used as a cellular tracking label in static images [18]. In addition to fluorescence properties, ND particles with the magnetic property may be developed as a contrast reagent for magnetic-resonance imaging (MRI). It has been reported that nitrogen (^{15}N) and carbon (^{12}C) ion implantations with implant energy of 100 keV on NDs can produce magnetism in ND particles [42]. Furthermore, magnetic nanoparticles can be conjugated on the surface of ND [21,43].

Although a theory postulating that endocytic ND clusters can be segregated during cell division and remain as a single ND cluster [17], there is currently no report on methods for separating ND-labeled cells and whether such labeled cell lines survive or have the ability to be sub-cultured. In present study, we develop the ND-bearing cancer cell lines using the fluorescent and magnetic nanodiamond (FMND) particles. It is successfully separated the FMND-bearing cells by flow cytometer or magnetic device. The FMND-bearing cells can be characterized and detected by flow cytometer and confocal microscope; more importantly, these FMND-bearing cells reserve cell viability and growth ability without altering cellular functions by comparing with the parental cells. The generations of FMND-bearing cancer cells can be applied for specific cancer cells on the labeling and tracking.

2. Materials and methods

2.1. Preparation of FMNDs

The fluorescent and magnetic nanodiamond, which called FMND, was synthesized as described previously [21]. Specifically, magnetic nanodiamond (MND) was composed of pristine ND and iron nanoparticle (ferrocene) via a microwave-arcing process. The ferrocene particles and NDs formed MNDs by chemically bonding. To introduce fluorescence in MNDs, MNDs were converted into FMNDs by covalent surface grafting with polyacrylic acids and fluorescein o-methacrylate. FMND particles were dissolved in distilled deionized water (DDW) or phosphate-buffered saline (PBS), before the treatment of cells using FMNDs.

2.2. Dynamic light scattering

The stock solution of 2.1 mg/ml FMND particles was prepared using DDW or PBS. To examine the size distribution of FMNDs dissolved in DDW and PBS, the concentration of FMND particles in DDW or PBS (0.5 mg/ml) was prepared and analyzed by DLS (BI-200SM, Brookhaven Instruments Co., Holtsville, NY). In a particular suspension, when a beam of laser hits the particle, the particles scattered some of the laser. The measured data were subjected to the BIC dynamic light scattering software (Brookhaven Instruments Co.). The scattered light changed over time, and the average particle size was calculated by the variation of scattered light.

2.3. Cell culture

HFL-1 cells (ATCC #CCL-153) were normal lung fibroblasts derived from a Caucasian fetus. The A549 lung epithelial cell line (ATCC #CCL-185) was derived from the lung adenocarcinoma of a 58 year old Caucasian male. RKO was colon carcinoma cell line. BFTC905 cells were derived from bladder carcinoma. MCF-7 was a breast cancer cell line. HeLa was a cervix cancer cell line. HFL-1 and HeLa cells were maintained in DMEM medium (Invitrogen Co., Carlsbad, CA). A549, BFTC905, MCF-7 cells were maintained in RPMI-1640 medium (Invitrogen). The complete media contained 10% fetal bovine serum (FBS), 100 unit/ml penicillin and 100 μ g/ml streptomycin. These cells were incubated at 37 °C, and maintained in 5% CO_2 in a humidified incubator (310/Thermo, Forma Scientific, Inc., Marietta, OH).

2.4. MTT assays

The cells were plated in 96-well plates at a density 1×10^4 cells/well for 16–20 h. The cells were treated with or without FMNDs for 24 h in complete medium. Subsequently, the medium was replaced and the cells were incubated with 0.5 mg/ml of 3-(4,5-dimethyl-thiazol-2-yl)-2,5-diphenyl tetrazolium bromide (MTT) (Sigma Chemical Co., St. Louis, MO) in complete medium for 4 h. The surviving cells converted MTT to formazan, which generates a blue-purple color when dissolved in dimethyl sulfoxide (DMSO). The intensity of formazan was measured at 565 nm using a plate reader (VERSAmax, Molecular Dynamics Inc., CA) for enzyme-linked immunosorbent assays. Cell viability was calculated by dividing the absorbance of the cells treated with FMNDs by that of the cells not treated with FMNDs.

2.5. Cell growth assays

A549 cells were seeded at a density of 1×10^6 cells per 100-mm Petri dish in complete medium for 24 h. Then, the cells were treated with or without FMNDs (50 μg/ml) for 24 h. Subsequently, the cells treated or untreated with FMNDs were re-cultured in fresh medium for counting the total cell number every 2 days, for a total of 10 days.

2.6. Cellular fluorescence intensity, particles complexity and size distribution by FMNDs

A549 cells were plated at a density of 7×10^5 cells per 60-mm Petri dish in complete medium for 16–20 h. After treatment in medium with or without FMNDs, the cells were washed twice with PBS. The cells were trypsinized and collected by centrifugation at 1500 rpm for 5 min. Thereafter, the cell pellets were re-suspended in PBS. To avoid cell aggregation, the cell suspension was filtered through a nylon mesh membrane. Finally, the samples were analyzed by flow cytometer (FACSCalibur, Becton–Dickinson, San Jose, CA). A minimum of 10,000 cells were analyzed. The fluorescence of FMNDs was excited at a wavelength of 488 nm, and was collected in the green light signal range. The fluorescence intensity, particle complexity and cell size were quantified using a minimum of 10,000 cells by CellQuest software (BD Biosciences).

2.7. Immunofluorescence staining and confocal microscopy

The cells were cultured on cover slips, and kept in a 35-mm Petri dish for 16–20 h before treatment. After treatment with or without FMNDs, the cells were washed with isotonic PBS (pH 7.4), and then were fixed with 4% paraformaldehyde solution in PBS for 1 h at 37 °C. Thereafter, the cover slips were washed three times with PBS and non-specific binding sites were blocked in PBS containing 10% FBS, 0.3% Triton-X-100 for 1 h. The β-tubulin and nuclei were stained with anti-β-tubulin Cy3 (1:100) and Hoechst 33258 (Sigma Chemical Co., St. Louis, Mo) for 30 min at 37 °C, respectively. Finally, the samples were examined under an OLYMPUS confocal microscope (FV500, OLYMPUS, Japan) or Confocal Microscope System (TCS-SP5-X AOBS, Leica, Germany).

2.8. Separation of FMND-bearing cells by a flow cytometer

The protocol of separating FMND-bearing cells by flow cytometer shows in supplementary protocol 1. Briefly, the cells were plated at a density of 2×10^6 cells per 100-mm Petri dish in complete medium for 24 h. After treatment with FMNDs (50 μg/ml) for 24 h, the cells were washed twice with PBS. The washed cells were trypsinized and collected by centrifugation at 1500 rpm for 5 min. Thereafter, the cell pellets were re-suspended in 1–2 ml ice-cold sorting buffer, which contained 1 mM EDTA, 25 mM HEPES and 2% FBS in PBS. To avoid cell aggregation, the cell suspension was filtered through a nylon mesh membrane. The fluorescence-activated cell-sorting analyses were performed with a FACSCalibur with a sorter (Becton–Dickinson). The FMND-bearing cells, which displayed green fluorescence intensity in flow cytometer, were selected for separation. The separated cells were collected in a 50 ml centrifuge tube that had been coated with 10% FBS on the wall

was collected in 515–545 nm signal range (FL1-H). FSC-H indicates the cell size distribution. (B) *Y*-axis indicates the cell counts. FSC-H indicates the cell size distribution. (C) The cell size distribution of FSC-H was quantified from a minimum of 10,000 cells by CellQuest software. Results were obtained from three separate experiments and the bar represents mean ± S.E. (D) The cells were incubated with or without 50 μg/ml FMND for 0–24 h. The fluorescence intensity from FMNDs was excited with wavelength 488 nm and the emission was collected in 515–545 nm signal range (FL1-H). FSC-H indicates the cell size distribution. (E) *Y*-axis indicates the cell counts. FSC-H indicates the cell size distribution. (F) The cell size distribution of FSC-H was quantified from a minimum of 10,000 cells by CellQuest software. Results were obtained from three separate experiments and the bar represents mean ± S.E.

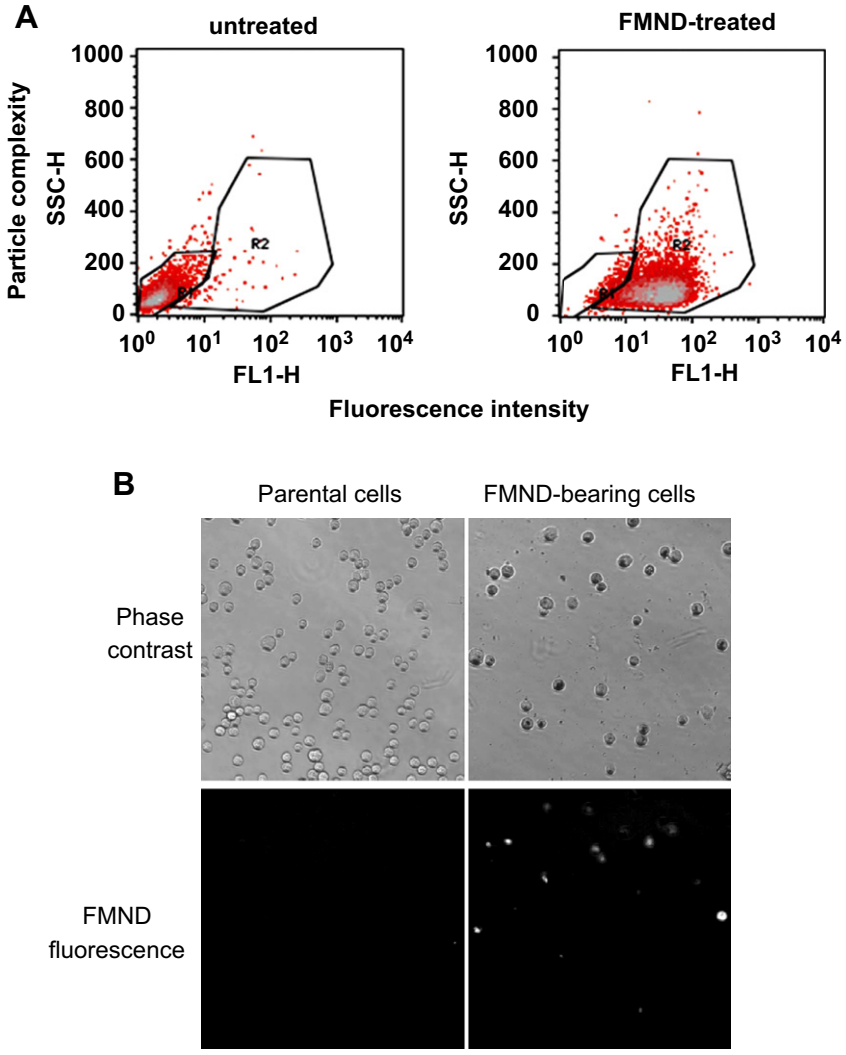

Fig. 5. Separation of the FMND-bearing cells by flow cytometer with a sorter. (A) A549 cells were plated at a density of 2×10^6 cells per 100-mm Petri dish for 24 h. Then the cells were incubated with 50 μg/ml of FMND for 24 h. After FMNDs treatment, the cells were collected in sorting buffer, and the FMND-bearing cells were separated by flow cytometer. The R1 gate indicates the region of control (green fluorescence-negative) cells. The R2 gate indicates the region of FMND-bearing (fluorescence-activated) cells. (B) After separation by flow cytometer, the cells were immediately observed under a living cell imaging system with a fluorescent and phase contrast microscope (40× magnification). The fluorescence from the FMNDs was excited with 488 nm, and the emission collected in the range of 510–530 nm.

and contained 15–20 ml of complete medium inside. After separation, the cell suspensions were centrifuged at 1000 rpm for 10 min. Then, the cell pellets were re-suspended in complete medium. The cells were incubated at 37 °C, in 5% CO_2 in a humidified incubator, or added 10% DMSO for storage in liquid nitrogen.

2.9. Separation of FMND-bearing cells by a magnetic device

The protocol of separating FMND-bearing cells by magnetic device shows in supplementary protocol 2. Briefly, the cells were plated at a density of 2×10^6 cells per 100-mm Petri dish in complete medium for 24 h. After treatment with 50 μg/ml FMNDs for 24 h, the cells were washed twice with PBS. The washed cells were trypsinized, and collected by centrifugation at 1500 rpm for 5 min. The cell pellets were re-suspended in 1 ml PBS and transferred to 1.5 ml eppendorf tubes. The eppendorf tubes were placed onto a magnetic rack (Magna GrIP Rack, Millipore, Bedford, MA) for at least 3 min, until the cell pellets were absorbed on the tube walls. Then, the suspensions were removed, and the cell pellets were dissolved in complete medium. The cell suspensions with the eppendorf tubes were repeatedly placed onto the magnetic rack 5 times. Finally, the FMND-bearing cells were incubated at 37 °C, and in 5% CO_2 in a humidified incubator, or added 10% DMSO for storage in liquid nitrogen.

2.10. SDS-PAGE analysis

To compare the total protein expression profiles between the parental and FMND-bearing cells, the cells were subjected to sodium dodecyl sulfate polyacrylamide gel electrophoresis (SDS-PAGE) analysis. The separated FMND-bearing cells were lysed in the ice-cold cell extraction buffer (pH 7.6), which contained 0.5 mM DTT, 0.2 mM EDTA, 20 mM HEPES, 2.5 mM $MgCl_2$, 75 mM NaCl, 0.1 mM Na_3VO_4, 50 mM NaF, 0.1% Triton-X-100. The protease inhibitors included 1 μg/ml aprotinin, 0.5 μg/ml leupeptin and 100 μg/ml 4-(2-aminoethyl) benzenesulfonyl-fluoride were added to the cell suspension. The cell extracts were gently rotated at 4 °C for 30 min. After centrifugation, the pellets were discarded, and the supernatant protein concentrations were determined by a BCA protein assay kit (Pierce, Rockford, IL). Equal amounts of proteins (40 μg) were subjected to electrophoresis by 12% SDS-PAGE. After electrophoresis, the gel was stained with a coomassie blue buffer (0.1% coomassie blue, 10% acetic acid and 45% methanol) for 1 h.

2.11. Statistic analysis

Data was analyzed using Student's t-test, and a p value < 0.05 was considered as statistically significant in the experiments.

3. Results

3.1. Size distribution of FMNDs in DDW and PBS

The stock solution of 2.1 mg/ml FMND particles was prepared using DDW or PBS in tubes, and observed by immobilized for

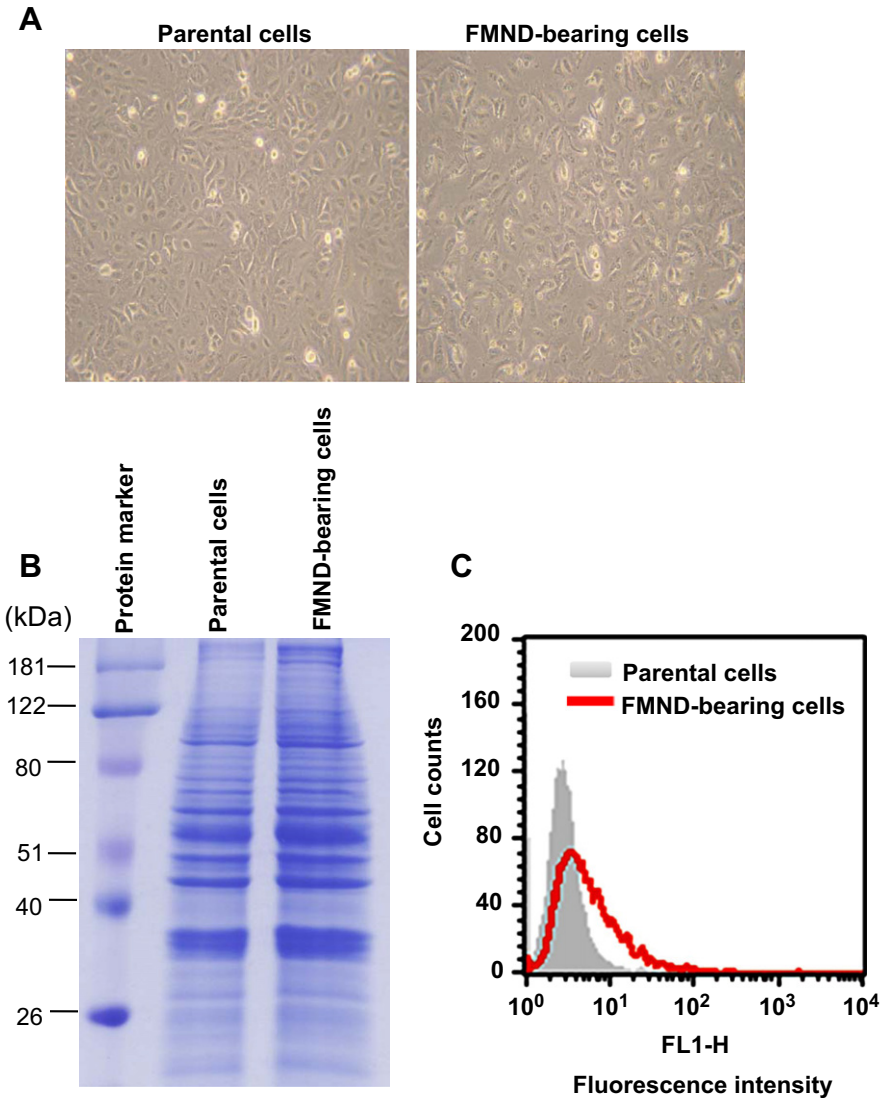

Fig. 6. Comparison of cell viability and total protein expression profiles between the parental and FMND-bearing cancer cells. (A) A549 cells were plated at a density of 2×10^6 cells per 100-mm Petri dish for 24 h. Then the cells were incubated with 50 μg/ml of FMND for 24 h. At the end of treatment, the FMND-bearing cells were separated by flow cytometer. After separation, the cells were re-cultured in fresh medium for 24 h. Representative phase contrast photomicrographs (40× magnification) show that cell morphology and viability in the parental cells and FMND-bearing cells. (B) Total protein expression profiles were compared between the parental and FMND-bearing cells. At the end of incubation, the total protein extracts were prepared for SDS-PAGE analysis. The left lane indicates the loading marker of proteins. (C) After separation, the FMND-bearing cells were re-cultured in fresh medium for 24 h. The fluorescence from FMND was excited with wavelength 488 nm and the emission was collected in 515–545 nm signal range (FL1-H) by flow cytometer.

0–24 h. Fig. 1A shows that FMNDs in DDW formed precipitates in the bottom of tubes after 2 h observation. FMNDs in PBS did not significantly cause aggregates after 24 h observation (Fig. 1A). To measure the size distribution of FMNDs, 0.5 mg/ml of FMND solution prepared in DDW or PBS was analyzed by DLS. The first peak of FMNDs in PBS was from 95.22 to 116.34 nm, and the second peak was from 272.58 to 333.04 nm (Fig. 1B, orange lines). The average size of FMNDs in PBS was 131.7 nm. The first peak of FMNDs in DDW was from 137.24 to 176.71 nm, and the second peak was from 805.15 to 1127.86 nm (Fig. 1B, green lines). The average size of FMNDs in DDW was 277.7 nm.

3.2. No significant cytotoxicity and cell growth inhibition by FMNDs in HFL-1 normal fibroblasts and A549 lung cancer cells

To examine cytotoxicity following treatment with FMMDs in human lung cells, HFL-1 normal fibroblasts and A549 human lung carcinoma cells were used. The cells were treated with FMNDs, and analyzed by MTT assays. As shown in Fig. 1C, HFL-1 normal fibroblasts treated with FMNDs (0.1–100 μg/ml, 24 h) did not significantly reduce cell viability. Similarly, FMND particles did not induce cytotoxicity in A549 cells (Fig. 1D). The cell growth ability was analyzed after treatment with or without 50 μg/ml FMND particles for 24 h in A549 cells, and then further cultured for another 10 days. The total cell number was counted every 2 days. Fig. 1E shows that FMND particles did not alter the cell growth ability in A549 cells. Using DDW or PBS as an FMND solvent had no significantly altered the cell viability and cell growth ability (Fig. 1C–E). To prepare the FMND-bearing cancer cells, PBS was used as a solvent for FMND particles in this study.

3.3. Fluorescence intensity, particle complexity and size distribution of A549 lung cancer cells after treatment with FMNDs

The fluorescence intensity of FMNDs in A549 cells was examined by flow cytometer. Treatment with FMNDs (10–100 μg/

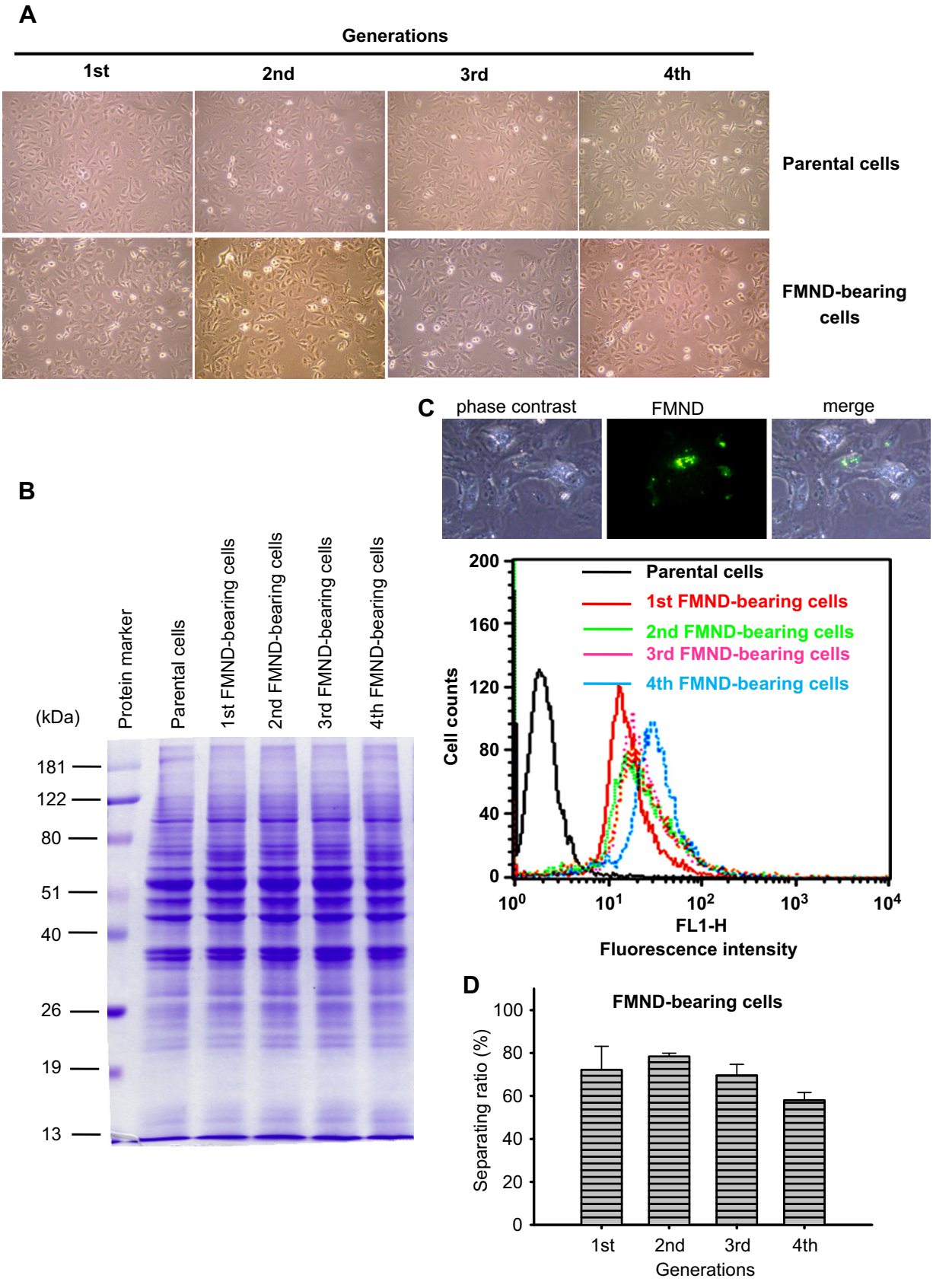

Fig. 7. Comparison of cell morphology, viability, total protein expression profile, and fluorescence intensity in the parental and FMND-bearing cells with various generations. (A) A549 cells were plated at a density of 2×10^6 cells per 100-mm Petri dish for 24 h. Then the cells were incubated with 50 μg/ml of FMNDs for 24 h. At the end of treatment, the 1st generation of FMND-bearing cells was separated by magnetic device. After separation, the FMND-bearing cells were re-cultured in fresh medium for 24 h. Thereafter, the cells were subjected to magnetic device for separation of the 2nd generation of FMND-bearing cells. The same protocol was repeated to separate the 3rd and 4th generations of FMND-bearing

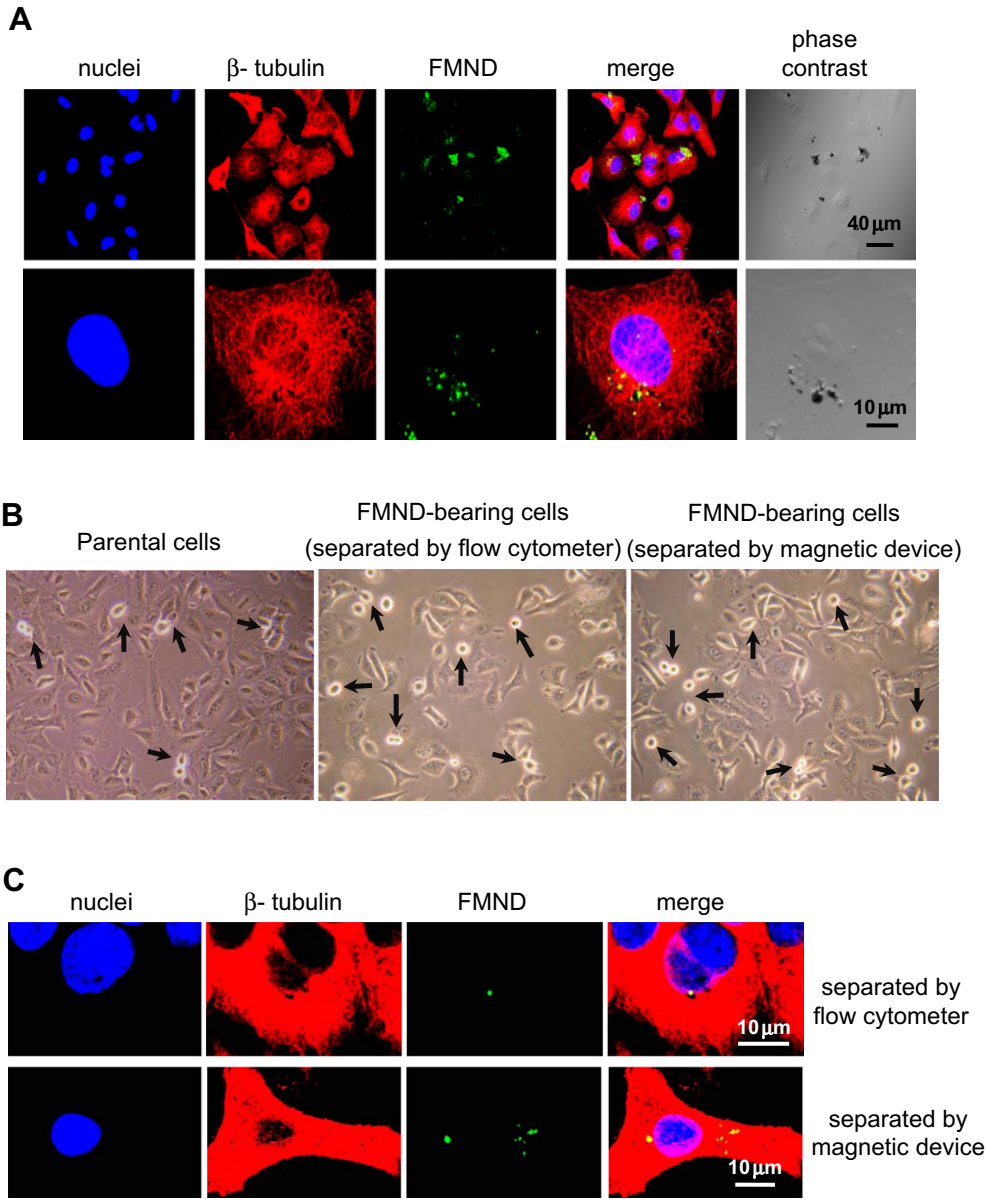

Fig. 8. Comparison of cell morphology and viability between the parental cells and re-thawed FMND-bearing cells. (A) A549 cells were plated at a density of 2×10^6 cells per 100-mm Petri dish for 24 h. Then the cells were incubated with 50 μg/ml of FMNDs for 24 h. At the end of treatment, the FMND-bearing cells were separated by magnetic device. After separation, the FMND-bearing cells were re-cultured on cover slips with fresh medium for 24 h. At the end of incubation, the cells were fixed and stained with the Cy3-labeled anti-β-tubulin and Hoechst 33258. The green fluorescence from the FMNDs was excited with 488 nm, and the emission collected in the range of 510–530 nm. The β-tubulin protein displayed red fluorescence. The nuclei were stained with Hoechst 33258, which displayed blue fluorescence. (B) The FMND-bearing A549 cell lines separated by flow cytometer or magnetic device were stored in liquid nitrogen. The cryopreservation of FMND-bearing cells was re-thawed in complete medium. The cell morphology, viability and growth ability were observed under a phase contrast microscope (40× magnification). The round-up cells (the arrows) indicate that the cells are undergoing cell division. (C) The FMND-bearing cells separated by flow cytometer or magnetic device were re-cultured for a further 7 days. The FMND particles exhibited green fluorescence inside A549 cells.

ml for 24 h) in A549 cells increased the fluorescence intensities of the cells (Fig. 2A). The quantified data showed that the fluorescence intensities of FMNDs inside A549 cells were in a concentration-dependent manner (Fig. 2B). The intracellular particle complexities of FMNDs in A549 cells were examined by SSC-H (lateral light scatter) using flow cytometer analysis. Treatment with FMNDs (10–100 μg/ml for 24 h) increased the intracellular particle complexities of A549 cells (Fig. 2C and D). The quantified data showed that the intracellular particle complexities of FMNDs in A549 cells were in a concentration-dependent manner (Fig. 2E). Besides, treatment with FMNDs (50 μg/ml) for a time-course (0.5–24 h) in A549 cells increased both the fluorescence intensities (Fig. 3A and C) and the intracellular particle complexities (Fig. 3C and D). The quantified data showed that

cells. The cell morphology, viability, and growth ability of FMND-bearing cells with different generations were observed under a phase contrast photomicroscope (40× magnification). (B) The total protein extracts from the parental cells and FMND-bearing cells were prepared for SDS-PAGE analysis. The left lane indicated the loading marker of proteins. (C) The different generations of FMND-bearing cells were separated by magnetic device. The green fluorescence of FMNDs in cells was detected by a living cell imaging system or flow cytometer. (D) A549 cells were plated at a density of 2×10^6 cells per 100-mm Petri dish for 24 h. Then the cells were incubated with 50 μg/ml of FMNDs for 24 h. Different generations of FMND-bearing cells were separated by magnetic device. The separating ratio of FMND-bearing cells is calculated by separated cell number from magnetic device dividing to total counted cell number before separation.

fluorescence intensities (Fig. 3B) and particle complexities (Fig. 3E) were significantly increased following FMNDs in A549 cells via a time-dependent manner. Nonetheless, treatment with FMNDs (10–100 μg/ml for 24 h) in A549 cells did not alter the cell size distribution by FSC-H (forward light scatter) analysis using flow cytometer (Fig. 4A and B). Consistently, FMNDs (50 μg/ml) for a time-course (0.5–24 h) did not alter the cell size distribution of A549 cells (Fig. 4D and E). The quantified data showed that the cell size distribution of A549 cells was not significantly altered after treatment with FMNDs (Fig. 4C and F, $p > 0.05$).

3.4. Identification of the FMND-bearing cells separated by flow cytometer

Separation of the FMND-bearing cells by flow cytometer was described in supporting information (please see the supplementary protocol 1). To separate the FMND-bearing cells, A549 cells were treated with or without FMNDs (50 μg/ml for 24 h). The R1 gate (green fluorescence-negative) indicates the region of parental cells (Fig. 5A). The R2 gate (green fluorescence-active) indicates the region of the FMND-bearing cells that displayed the green fluorescence intensities (Fig. 5A). The FMND-bearing cells in the R2 region were collected by the flow cytometer with a sorter. After separation, the FMND-bearing cells were immediately examined under a living cell imaging system with a fluorescent and phase contrast microscope. Comparison with the parental cells shows that the separated FMND-bearing cells exhibited significant fluorescence intensity under a fluorescent microscope (Fig. 5B, right lower picture). Moreover, the FMND-bearing cells were re-cultured for a further 24 h. The cell morphology and viability were observed under a phase contrast microscope. The viability and growth ability of FMND-bearing cells were similar to the parental cells by observing confluent cells in culture dishes (Fig. 6A). Subsequently, the total protein expression profiles of the FMND-bearing cells and parental cells were examined by SDS-PAGE analysis. The protein expression patterns on the SDS-PAGE were not significantly altered between the parental cells and FMND-bearing cells (Fig. 6B). Besides, the green fluorescence intensities in the FMND-bearing cells could be distinguished by flow cytometer after the cells were cultured for a further 24 h (Fig. 6C, red peak in web version).

3.5. Identification of the FMND-bearing cells separated by magnetic device

Separation of the FMND-bearing cells by magnetic device was described in supporting information (please see the supplementary protocol 2). To collect the FMND-bearing cells, A549 cells were treated with FMNDs (50 μg/ml for 24 h), and separated by magnetic device. The cell morphology, viability and growth ability of the FMND-bearing cells with different generations separated by magnetic device were similar to the parental cells (Fig. 7A). In addition, the protein expression patterns of FMND-bearing cells on the SDS-PAGE were not significantly altered (Fig. 7B). Moreover, the FMND-bearing cells still carried the fluorescence intensities of FMNDs, and that these fluorescence intensities could be detected by flow cytometer (Fig. 7C, lower picture) or confocal microscope (Fig. 7C, upper picture).

The separating ratio of the generations of FMND-bearing cells was calculated by dividing the separated FMND-bearing cell number by total counted cell number before separation. The separating ratio of the first generation had an average of 75.89%, and the separating ratio in the fourth generation had an average of ~60% (Fig. 7D).

3.6. Cryopreservation and characterization of the generations of FMND-bearing cells separated by flow cytometer or magnetic device

The first generation of the FMND-bearing cells separated by flow cytometer or magnetic device was cryopreservation in liquid nitrogen. After re-thawing the FMND-bearing cells, the cells were observed by laser scanning confocal microscope. The nuclei were stained with Hoechst 33258 that presented with blue color. The red fluorescence (Cy3) exhibited by β-tubulin that presented the cell morphology (cytoskeleton) of A549 cells. The FMND particles exhibited green fluorescence in A549 cells at wavelength 488 nm, and the emission collected in the range of 510–530 nm (Fig. 8A). The images of phase contrast showed the location of FMNDs retained in A549 cells (Fig. 8A, dark black spots). The cell morphology and viability of the FMND-bearing cells were still similar to those of the parental cells (Fig. 8B). The arrows in Fig. 8B indicate round-up cells undergoing cell division. Moreover, the FMND's particles retained inside of the FMND-bearing cells after the cells were cultured for a further 7 days (Fig. 8C).

3.7. Separation and identification of various FMND-bearing cancer cell types

A variety of cancer cell types have been examined for illustrating universal of the FMND-bearing cells. Human cancer cell lines including human colon (RKO), bladder (BFTC905), breast (MCF-7), and cervix (HeLa) were incubated with FMND particles (50 μg/ml for 24 h), and then the FMND-bearing cells were separated by magnetic device. The fluorescence intensities of FMNDs in various cancer cell types were examined by flow cytometer. All cell lines were increased the fluorescence intensities following treatment with FMNDs (Fig. 9A). The quantified data showed that the fluorescence intensities of FMNDs were significantly increased in all cell lines (Fig. 9A). The FMND-bearing cancer cell lines were confirmed by confocal microscope by which retained the FMND particles that exhibited green fluorescence (Fig. 9B).

4. Discussion

NDs have been developed in biological applications in recent years. In this study, we demonstrate the FMND-bearing cancer cell lines, which can be separated by flow cytometer and magnetic device. The FMND-bearing cells can be characterized and detected by flow cytometer and confocal microscopy. More importantly, the FMND-bearing cells reserved cellular functions, including cell morphology, cell viability and growth ability by comparison with the parental cells. In addition, a variety of human cancer types including lung (A549), colon (RKO), breast (MCF-7), cervical (HeLa), and bladder (BFTC905) cancer cells can be used the strategy to prepare the FMND-bearing cancer cell lines. These ND-bearing cell lines can be cryopreservation for further biomedical applications such as cellular labeling and tracking in cancer or stem cells.

NDs can be taken into A549 lung cancer cells by endocytosis [17]. The endocytic ND's clusters in cells were separated by cell division; finally, the cell retained a single ND's cluster [17]. Quantum measurement and orientation tracking of fluorescent NDs were used by the controlled single spin probes for nano-magnetometry inside living cells [44]. We found that treatment with FMNDs increased the fluorescence intensity and particle complexity of cancer cells in a concentration- and time-dependent manner but did not alter the cellular size distribution. Several studies show that NDs do not induce cytotoxicity in a variety of cell types [16–21]. It has been found that NDs did not cause significant abnormality in the cellular functions, including cell division and

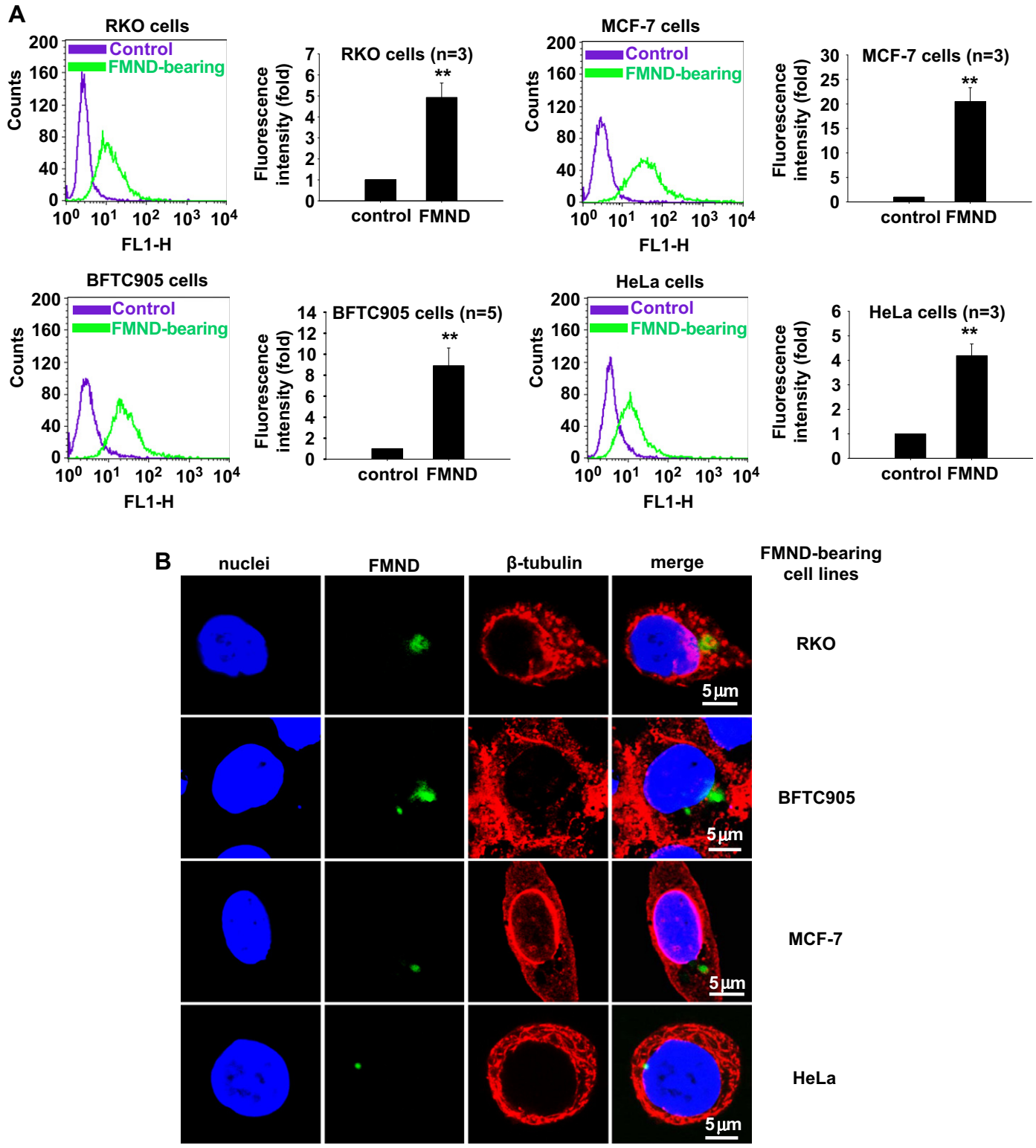

Fig. 9. Separation and identification of various FMND-bearing cancer cell types. (A) A variety of cancer cell lines including human colon (RKO), bladder (BFTC905), breast (MCF-7) and cervix (HeLa) cancer cells were plated at density of 2×10^6 cells per 100-mm Petri dish for 24 h. Then the cells were treated with or without 50 μg/ml FMNDs for 24 h. At the end of treatment, the cells were separated by magnetic device. The fluorescent intensity of FMNDs in the cells was detected by flow cytometer. The fluorescence intensity from FMNDs was excited with wavelength 488 nm, and emission was collected in 515–545 nm signal range. The fluorescence intensity was quantified from a minimum of 10,000 cells by CellQuest software. Result were obtained from 3 to 5 separate experiment and bar represent mean ± S.E. $^*p < 0.05$ indicates significant different between control and FMND-treated samples. (B) The FMND-bearing cells were subjected to nuclear and microtubule staining, and observed by laser scanning confocal microscope. The microtubule was stained with anti-β-tubulin Cy3 that presented with red color. The nuclei were stained with Hoechst 33258 that presented with blue color. The green fluorescence from FMND's particles was excited with wavelength 488 nm, and the emission was collected in the range of 510–530 nm. (For interpretation of the references to color in this figure legend, the reader is referred to the web version of this article.)

Table 1
Characterization of the FMND-bearing cancer cells separated by flow cytometer or magnetic device.

Separation methods	Cell morphology[a]	Cell viability[a]	Cell growth[a]	Total protein expression profile[b]	Cell lines storage[c]
Flow cytometer	Normal	Normal	Yes	Normal	Yes
Magnetic device	Normal	Normal	Yes	Normal	Yes

[a] Living cell morphology, cell viability and growth ability were examined under a phase contrast microscope by time-lapse observation and compared with the parental cells.
[b] The total protein expression profile was examined by SDS-PAGE analysis and compared with the parental cells.
[c] The separated FMND-bearing cell lines were frozen and stored in liquid nitrogen for further examinations or applications.

differentiation [17] and morphogenesis during embryogenesis [22]. FMNDs did not induce cytotoxicity and growth alteration in HFL-1 normal lung fibroblast and A549 lung cancer cells. These findings provided that FMNDs were carried inside of cells without inducing cellular damage. Accordingly, FMND is a biocompatible nanomaterial for establishing these ND-bearing cell lines.

FMNDs were with an aqueous solubility by stock solution at 2.1 mg/ml [21]. We found that PBS was more suitable solvent for FMNDs in the present study. The average size of FMNDs in PBS was 131.7 nm. We suggest that the functional groups on the surface of FMND particles may provide more solubility for FMNDs in the PBS buffer system. According to solubility, PBS was used as a solvent for FMND particles for preparing the FMND-bearing cells. Moreover, using DDW or PBS as an FMND solvent did not alter the cell viability and growth ability in human cells. The results indicate that different size of FMNDs does not induce cytotoxicity in human cells.

FMNDs contained both the advantages of fluorescence and magnetic properties for cancer cell labeling and detection. The fluorescence intensity of FMNDs provides for the separation of the ND-bearing cells by flow cytometer with cell-sorting function. The FMND-bearing cells were distinguished by fluorescence intensity of FMND particles using flow cytometer. In addition, the FMND-bearing cells can be separated by magnetic device. It has been used flow cytometer to get the fluorophore-conjugated iron oxide nanoparticle (Feridex)-labeled human hematopoietic stem cells [5]. After separation by flow cytometer or magnetic device, these FMND-bearing cells displayed cell survival and growth ability. Moreover, the morphology and total protein expression profiles of the FMND-bearing cells were similar to those of the parental cells.

The labeled or separated cells have cell morphology, viability and growth ability similar to those of the parent cells after subculturing or cryopreservation. The separating ratio of the generations of FMND-bearing cells was calculated by dividing the separated FMND-bearing cell number by total counted cell number before separation. We found that the separating ratio of the generations of FMND-bearing cells around 60–75%. It is possible that partial FMND-bearing cells may be lost during separation procedure. However, over 60% separation ratio of the fourth generation of the FMND-bearing cells can provide enough cell number for identification and application.

The characterization of FMND-bearing cells separated by flow cytometer and magnetic device was summarized in Table 1. These FMND-bearing cell lines can be cryopreservation and stored in liquid nitrogen for further biological applications such as specific cancer cell labeling and tracking. The FMND-bearing cancer cells may provide for cancer tracking by optical imaging or MRI detection in animals. Moreover, the FMND-bearing cancer cell lines can be used for anti-cancer drugs screening or other biomedical applications.

5. Conclusions

We have established the FMND-bearing cancer cell lines separated by flow cytometer and magnetic device without inducing cellular damages. The FMND-bearing cancer cell lines reserve the cellular functions similar to those of the parental cells that can provide for specific cancer cell labeling and tracking.

Acknowledgments

This work was supported by grants from the National Science Council (NSC 96-2311-B-320-006-MY3 and NSC 99-2311-B-009-003-MY3) and the National Chiao-Tung University (100W976) in Taiwan. The authors also thank the core facility of Multiphoton and Confocal Microscope System in National Chiao University, Hsinchu, Taiwan.

Appendix A. Supplementary material

Supplementary material associated with this article can be found, in the online version, at doi:10.1016/j.biomaterials.2012.05.009.

References

[1] Chithrani BD, Ghazani AA, Chan WC. Determining the size and shape dependence of gold nanoparticle uptake into mammalian cells. Nano Lett 2006;6(4):662–8.
[2] Alivisatos P. The use of nanocrystals in biological detection. Nat Biotechnol 2004;22(1):47–52.
[3] Lasne D, Blab GA, Berciaud S, Heine M, Groc L, Choquet D, et al. Single nanoparticle photothermal tracking (SNaPT) of 5-nm gold beads in live cells. Biophys J 2006;91(12):4598–604.
[4] Erogbogbo F, Yong KT, Roy I, Hu R, Law WC, Zhao W, et al. In vivo targeted cancer imaging, sentinel lymph node mapping and multi-channel imaging with biocompatible silicon nanocrystals. ACS Nano 2010;5(1):413–23.
[5] Maxwell DJ, Bonde J, Hess DA, Hohm SA, Lahey R, Zhou P, et al. Fluorophore-conjugated iron oxide nanoparticle labeling and analysis of engrafting human hematopoietic stem cells. Stem Cells 2008;26(2):517–24.
[6] Ruan J, Shen J, Wang Z, Ji J, Song H, Wang K, et al. Efficient preparation and labeling of human induced pluripotent stem cells by nanotechnology. Int J Nanomedicine 2011;6:425–35.
[7] Chen Y, Zhu X, Zhang X, Liu B, Huang L. Nanoparticles modified with tumor-targeting scFv deliver siRNA and miRNA for cancer therapy. Mol Ther 2010;18(9):1650–6.
[8] Batist G, Ramakrishnan G, Rao CS, Chandrasekharan A, Gutheil J, Guthrie T, et al. Reduced cardiotoxicity and preserved antitumor efficacy of liposome-encapsulated doxorubicin and cyclophosphamide compared with conventional doxorubicin and cyclophosphamide in a randomized, multicenter trial of metastatic breast cancer. J Clin Oncol 2001;19(5):1444–54.
[9] Liu Z, Chen K, Davis C, Sherlock S, Cao Q, Chen X, et al. Drug delivery with carbon nanotubes for in vivo cancer treatment. Cancer Res 2008;68(16):6652–60.
[10] Krueger A. New carbon materials: biological applications of functionalized nanodiamond materials. Chemistry 2008;14(5):1382–90.
[11] Schrand AM, Hens SAC, Shenderova OA. Nanodiamond particles: properties and perspectives for bioapplications. Crit Rev Solid State Mat Sci 2009;34(1–2):18–74.
[12] Mochalin VN, Shenderova O, Ho D, Gogotsi Y. The properties and applications of nanodiamonds. Nat Nanotechnol 2011;7(1):11–23.
[13] Krueger A, Stegk J, Liang Y, Lu L, Jarre G. Biotinylated nanodiamond: simple and efficient functionalization of detonation diamond. Langmuir 2008;24(8):4200–4.
[14] Bouzigues C, Gacoin T, Alexandrou A. Biological applications of rare-earth based nanoparticles. ACS Nano 2011;5(11):8488–505.
[15] Zhang XQ, Lam R, Xu X, Chow EK, Kim HJ, Ho D. Multimodal nanodiamond drug delivery carriers for selective targeting, imaging, and enhanced chemotherapeutic efficacy. Adv Mater 2011;23(41):4770–5.
[16] Liu KK, Cheng CL, Chang CC, Chao JI. Biocompatible and detectable carboxylated nanodiamond on human cell. Nanotechnology 2007;18:325102.

[17] Liu KK, Wang CC, Cheng CL, Chao JI. Endocytic carboxylated nanodiamond for the labeling and tracking of cell division and differentiation in cancer and stem cells. Biomaterials 2009;30(26):4249–59.
[18] Schrand AM, Lin JB, Hens SC, Hussain SM. Temporal and mechanistic tracking of cellular uptake dynamics with novel surface fluorophore-bound nanodiamonds. Nanoscale 2011;3(2):435–45.
[19] Yu SJ, Kang MW, Chang HC, Chen KM, Yu YC. Bright fluorescent nanodiamonds: no photobleaching and low cytotoxicity. J Am Chem Soc 2005; 127(50):17604–5.
[20] Vaijayanthimala V, Tzeng YK, Chang HC, Li CL. The biocompatibility of fluorescent nanodiamonds and their mechanism of cellular uptake. Nanotechnology 2009;20(42):425103.
[21] Chang IP, Hwang KC, Chiang CS. Preparation of fluorescent magnetic nanodiamonds and cellular imaging. J Am Chem Soc 2008;130(46):15476–81.
[22] Mohan N, Chen CS, Hsieh HH, Wu YC, Chang HC. In vivo imaging and toxicity assessments of fluorescent nanodiamonds in *Caenorhabditis elegans*. Nano Lett 2010;10(9):3692–9.
[23] Maitra U, Jain A, George SJ, Rao CN. Tunable fluorescence in chromophore-functionalized nanodiamond induced by energy transfer. Nanoscale 2011; 3(8):3192–7.
[24] Zhang Q, Mochalin VN, Neitzel I, Knoke IY, Han J, Klug CA, et al. Fluorescent PLLA-nanodiamond composites for bone tissue engineering. Biomaterials 2011;32(1):87–94.
[25] Hens SC, Cunningham G, Tyler T, Moseenkov S, Kuznetsov V, Shenderova O. Nanodiamond bioconjugate probes and their collection by electrophoresis. Diam Relat Mat 2008;17(11):1858–66.
[26] Zhang XQ, Chen M, Lam R, Xu XY, Osawa E, Ho D. Polymer-functionalized nanodiamond platforms as vehicles for gene delivery. ACS Nano 2009;3(9): 2609–16.
[27] Alhaddad A, Adam MP, Botsoa J, Dantelle G, Perruchas S, Gacoin T, et al. Nanodiamond as a vector for siRNA delivery to ewing sarcoma cells. Small 2011;7(21):3087–95.
[28] Hartl A, Schmich E, Garrido JA, Hernando J, Catharino SCR, Walter S, et al. Protein-modified nanocrystalline diamond thin films for biosensor applications. Nat Mater 2004;3(10):736–42.
[29] Tzeng YK, Faklaris O, Chang BM, Kuo Y, Hsu JH, Chang HC. Superresolution imaging of albumin-conjugated fluorescent nanodiamonds in cells by stimulated emission depletion. Angew Chem Int Ed Engl 2011;50(10):2262–5.
[30] Wang HD, Niu CH, Yang Q, Badea I. Study on protein conformation and adsorption behaviors in nanodiamond particle-protein complexes. Nanotechnology 2011;22(14):145703.
[31] Chao JI, Perevedentseva E, Chung PH, Liu KK, Cheng CY, Chang CC, et al. Nanometer-sized diamond particle as a probe for biolabeling. Biophys J 2007; 93(6):2199–208.
[32] Cheng CY, Perevedentseva E, Tu JS, Chung PH, Chenga CL, Liu KK, et al. Direct and *in vitro* observation of growth hormone receptor molecules in A549 human lung epithelial cells by nanodiamond labeling. Appl Phy Lett 2007;90: 163903.
[33] Huang LC, Chang HC. Adsorption and immobilization of cytochrome c on nanodiamonds. Langmuir 2004;20(14):5879–84.
[34] Nicolau E, Mendez J, Fonseca JJ, Griebenow K, Cabrera CR. Bioelectrochemistry of non-covalent immobilized alcohol dehydrogenase on oxidized diamond nanoparticles. Bioelectrochemistry 2012;85:1–6.
[35] Tran DT, Vermeeren V, Grieten L, Wenmackers S, Wagner P, Pollet J, et al. Nanocrystalline diamond impedimetric aptasensor for the label-free detection of human IgE. Biosens Bioelectron 2011;26(6):2987–93.
[36] Smith AH, Robinson EM, Zhang XQ, Chow EK, Lin Y, Osawa E, et al. Triggered release of therapeutic antibodies from nanodiamond complexes. Nanoscale 2011;3(7):2844–8.
[37] Liu KK, Zheng WW, Wang CC, Chiu YC, Cheng CL, Lo YS, et al. Covalent linkage of nanodiamond-paclitaxel for drug delivery and cancer therapy. Nanotechnology 2010;21(31):315106.
[38] Chow EK, Zhang XQ, Chen M, Lam R, Robinson E, Huang H, et al. Nanodiamond therapeutic delivery agents mediate enhanced chemoresistant tumor treatment. Sci Transl Med 2011;3(73):73ra21.
[39] Adnan A, Lam R, Chen H, Lee J, Schaffer DJ, Barnard AS, et al. Atomistic simulation and measurement of pH dependent cancer therapeutic interactions with nanodiamond carrier. Mol Pharm 2011;8(2):368–74.
[40] Li J, Zhu Y, Li W, Zhang X, Peng Y, Huang Q. Nanodiamonds as intracellular transporters of chemotherapeutic drug. Biomaterials 2010;31(32):8410–8.
[41] Barras A, Lyskawa J, Szunerits S, Woisel P, Boukherroub R. Direct functionalization of nanodiamond particles using dopamine derivatives. Langmuir 2011; 27(20):12451–7.
[42] Talapatra S, Ganesan PG, Kim T, Vajtai R, Huang M, Shima M, et al. Irradiation-induced magnetism in carbon nanostructures. Phys Rev Lett 2005;95(9): 097201.
[43] Gubin SP, Popkov OV, Yurkov GY, Nikiforov VN, Koksharov YA, Eremenko NK. Magnetic nanoparticles fixed on the surface of detonation nanodiamond microgranules. Diam Relat Mat 2007;16(11):1924–8.
[44] McGuinness LP, Yan Y, Stacey A, Simpson DA, Hall LT, Maclaurin D, et al. Quantum measurement and orientation tracking of fluorescent nanodiamonds inside living cells. Nat Nanotechnol 2011;6(6):358–63.